# Influence of polymerization pressure and post-cure treatment on conversion degree and viscoelastic properties of polymer infiltrated ceramic network

Benjamin Pomès, Pascal Béhin, Laurence Jordan, Stéphane Legoff, Gregory Stoclet, Emmanuel Richaud, Jean-François Nguyen

# Influence of polymerization pressure and post-cure treatment on conversion degree and viscoelastic properties of polymer infiltrated ceramic network

Benjamin Pomès [a,b], Pascal Behin [c], Laurence Jordan [a,d], Stéphane Legoff [e], Gregory Stoclet [f], Emmanuel Richaud [b], Jean-François Nguyen [a,d,*]

[a] UFR d'Odontologie Université de Paris, F-75006, Paris, France
[b] Arts et Métiers ParisTech, Laboratoire de Procédés et Ingénierie en Mécanique et Matériaux (PIMM), CNRS, CNAM, UMR, 8006, F-75013, Paris, France
[c] Université de Lille, Lille, France
[d] PSL Research University, Chimie ParisTech -CNRS, Institut de Recherche de Chimie Paris, F-75005, Paris, France
[e] Unité de Recherches Biomatériaux Innovants et Interfaces (URB2I-EA4462), Faculté de Chirurgie Dentaire, Université de Paris, Paris, France
[f] Université de Lille, CNRS, INRA, ENSCL, UMR 8207 - UMET - Unité Matériaux et Transformations, F-59000, Lille, France

*Keywords:*
CAD/CAM blocks
High-pressure polymerization
Dynamic mechanical analysis
Conversion degree

A B S T R A C T

This study aimed at determining an optimum polymerization pressure for Polymer Infiltrated Ceramic Network (PICN) blocks by characterizing the conversion degree (DC) and the viscoelastic properties of experimental PICN blocks polymerized at 90 °C under various high pressures followed or not by post-cure treatment (PC). Near infrared analysis and dynamic mechanical analysis were used to characterize DC and viscoelastic properties of sixteen PICN: one control (thermo-cured) and fifteen experimental groups (one thermo-cured followed by PC and fourteen high pressure polymerized PICN, in the range of 50–350 MPa without and with PC). Conversion degree of high pressure polymerized PICN blocks without post curing displays an optimum between 100 and 150 MPa resulting in an improved E′ and $T_g$. Post curing induces a higher DC with a controversial effect on thermo-mechanical properties. The results suggested that 100–150 MPa without PC is an optimum polymerization parameter, resulting in PICN blocks with significantly better DC, $T_g$, E'.

## 1. Introduction

Manufacturing of dental restoration has evolved from artisanal methods (using handmade buildup materials) to digital workflow with computer-aided design/computer-aided (CAD/CAM) process. Indeed, CAD/CAM systems are currently in full development making it possible to simplify the manufacturing steps (Miyazaki et al., 2009; Tallarico, 2020; Van Noort, 2012) and to use materials, such as ceramic or composite blocks that cannot be processed by artisanal methods (Mainjot et al., 2016). In comparison with ceramic blocks, composite blocks display an easier machinability, reduced machining time and wear of cutting tools (Ruse and Sadoun, 2014), together with good marginal adaptation (de Paula Silveira et al., 2017). Composite blocks have thus become an interesting choice as compared to ceramic blocks (Mainjot et al., 2016; Ruse and Sadoun, 2014).

Artisanal indirect composites are handmade buildups then photopolymerized, like conventional direct composites, and differ from composite blocks in the process manufacturing (artisanal handmade buildups vs industrial CAD/CAM blocks), polymerization method (photopolymerization vs high temperature -high pressure polymerization for composite blocks), microstructure (dispersed filler vs PICN or dispersed filler for composite blocks) (Mainjot et al., 2016). These parameters result in significant impacts on materials properties. Compared to artisanal composites, the homogeneity of CAD/CAM industrial composite blocks are better, with fewer flaws and pores (Giordano, 2006) but above all it allows overcoming an important drawback which is their incomplete polymerization because of more efficient polymerization methods. Indeed, conventional photopolymerization results in low DC (55–69%) (Al-Ahdal et al., 2015; Ferracane, 2011; Germscheid et al., 2018; Par et al., 2020). As DC is related to mechanical properties and monomer release, low DC results in poor mechanical properties (Ferracane, 2013), and biological risks because of the release of monomers in oral environment (Barutcigil et al., 2020; Bouillaguet, 2004). Polymerization under high temperature high pressure was shown to solve this issue by significantly increasing crosslinking, DC (up to 96% with an optimum at 200 MPa) (Phan et al., 2015), mechanical properties of

* Corresponding author. UFR d'Odontologie Université Paris Diderot, 5 rue, Garancière, 75006, France.
*E-mail address:* jean-francois.nguyen@u-paris.fr (J.-F. Nguyen).

UDMA polymer and its composites, and decrease the free monomer release (Phan et al., 2014).

Among composite blocks, two classes differ by their microstructure: dispersed fillers and polymer infiltrated ceramic network (PICN) (Mainjot et al., 2016; Sadoun, 2011). Concerning dispersed fillers composite blocks, filler particles are mixed with the monomer by mixing, and finally dispersed into the polymer matrix, then thermopolymerized with or without high pressure. PICN are made of sintered glass-ceramics porous network, silanated, secondarily infiltrated with monomer and then polymerized under high temperature high pressure (Mainjot et al., 2016).

Previous studies reported that PICN present better mechanical properties such as fracture toughness and flexural strength than conventional composites (M. Eldafrawy et al., 2018; Nguyen et al., 2014) and good biocompatibility (Barutcigil et al., 2020; Grenade et al., 2017; Tassin et al., 2016) because of the higher filler volume fraction ($V_f$) and their interpenetrating network technology (Coldea et al., 2013; He et al., 2011; Mainjot et al., 2016; Swain et al., 2016).

Indeed, the higher quantity of fillers decreases the ratio of resin and the quantity of resin in contact with saliva, reducing of the biodegradation rate, the leaching of unreacted monomers and degradation products (Bandarra et al., 2020; Cândea Ciurea et al., 2019; Finer and Santerre, 2007). It was indeed shown that commercial PICN tends to release no or very few monomers (Barutcigil et al., 2020; Putzeys et al., 2020). Moreover, PICN with their double-network microstructure resulting in a honeycomb polymer-based structure microstructure allows enhanced bonding properties compared to composite blocks with dispersed fillers microstructure (Eldafrawy et al., 2019; M Eldafrawy et al., 2018).

However, data concerning DC and viscoelastic properties of PICN are still missing. Viscoelastic properties of materials are often measured by dynamic testing, applying a sinusoidal force, calculating the resulting strain response and determining the elastic response E' (storage modulus) and the viscous response E'' (loss modulus). Values of E′ and E (elastic modulus) are very close although their determinations are not same. Indeed E′ is calculated from material response to a sinusoidal strain and E is the slope of the stress strain curve in the final linear region (Menard, 2008). This test can be performed at various temperature and determine glass transition temperature $T_g$ which depends on the network crosslink density (Menard, 2008). Dynamic mechanical analysis (DMA) test is very helpful to characterize dental resin composites as it allows to simulate the cyclic masticatory loading and so to predict the clinical performance of dental restorations. In particular, the damping factor tan δ (tan δ = E''/E') illustrates the capacity of the material to dissipate the energy (Al-shatti et al., 2019; Ong et al., 2018; Vouvoudi and Sideridou, 2013, 2012).

Nevertheless, in the case of composite materials, fillers induce an increase in viscosity and an earlier vitrification of material with a subsequent DC decrease (Leprince et al., 2013). Post-cure (PC) is hence used as a strategy to enhance DC (Par et al., 2019). It was shown to improve mechanical properties of dispersed fillers resin composites like elastic modulus (Almeida-chetti et al., 2014; Asmussen and Peutzfeldt, 1998), microhardness (Khan et al., 1993; Soares et al., 2005),diametral tensile strength (Asmussen and Peutzfeldt, 1990; Khan et al., 1993; Soares et al., 2005) and flexural strength (Asmussen and Peutzfeldt, 1990).

An understanding of the effect of pressure and PC polymerization on DC and viscoelastic properties of PICN is still lacking and would allow the optimization of the process for the purpose of large industrial production. Indeed, determining the optimum pressure of polymerization is mandatory as high pressure promotes two main effects on molecules during polymerization (Arita et al., 2008; Kojima et al., 2002). Increasing pressure brings the monomers closer, thus improving the reactivity (Arita et al., 2008; Kojima et al., 2002; Schettino et al., 2008) while at very elevated pressures, it would decrease the molecular mobility and slow down the polymerization kinetics for the polymerization of tetraethylene glycol dimethacrylate (Kaminski et al., 2008). Using a too high pressure of polymerization would hence have no benefit due to higher costs, stress and damage on autoclave.

As physical and chemical properties of dental restorative materials contribute to clinical success, characterizing their DC and viscoelastic properties is an interesting way to assess their behavior in oral cavity. The purpose of this study is to characterize the influence of pressure polymerization and post-cure on DC and viscoelastic of experimental PICN composite blocks, and to determine the optimal parameters polymerization regarding DC, E' and $T_g$. The null hypothesis tested was that varying polymerization pressure and PC have no effect on DC and on the viscoelastic properties of the high pressure polymerized PICN obtained in comparison with those of control, thermo-cured PICN composite blocks.

## 2. Materials and methods

### 2.1. Specimen preparation

Sixteen PICN groups, including one control group thermo-cured at ambient pressure without PC (TC), thermo-cured under various pressures ranging from 0.1 MPa and from 50 to 350 MPa with 50 MPa increments, without and with PC, were made using a previously described manufacturing process and same materials (Nguyen et al., 2014). The albite glass-ceramic networks were manufactured from VITA Mark II (VITA Zahnfabrik, Germany) with 5.13 μm D50 grain size distribution by slip casting process. The slurry was prepared by mixing 56% volume ratio glass-ceramic powder with deionized water in a planetary mixer (Thinky ARE-250, Thinky Corporation, Tokyo, Japan) and was cast in a plaster mold to get the grain agglomeration and then was dried and sintered at 800 °C for 2 h to obtain partially sintered blocks with open porosities. Silanazation was done with pre-hydrolyzed 3-(trimethoxysilyl) propyl methacrylate (Sigma Aldrich, Saint-Louis, USA) and heated at 140 °C for 6 h, and then infiltrated under vacuum with a mixture of 99.5% (wt) urethane dimethacrylate (UDMA; Esstech, USA) in the presence of 0.5% benzoyl peroxide (BPO; Sigma Aldrich, Steinheim, Germany) in this study.

Polymerization was performed at 90 °C, at various pressure (in range from 0.1 MPa to 350 MPa) following the procedure described previously (Phan et al., 2015) resulting in PICN blocks with dimensions of (13.2 ± 0.1) mm × (14.6 ± 0.1) mm × (22 ± 0.1) mm. Experimental conditions, reactants, polymerization parameters, and the group designation of the sixteen experimental PICN blocks made are summarized in Table 1.

Specimens for PICN monomer (19 mm × 12 mm × 1 mm) were made from uncured infiltrated glass-ceramic networks and were used for the determination of DC as PICN monomer. The control specimens (group TC) were produced from the infiltrated glass-ceramic networks thermally cured for 4 h at 90 °C under ambient pressure (0.1 MPa) in an oven (Memmert, Schwabach, Germany). The high pressure thermo-cured specimens (groups 50 to 350) were synthesized from the infiltrated glass-ceramic networks cured at 90 °C under high pressure ranging from 50 to 350 MPa with 50 MPa increments in a custom-built autoclave for 4 h. The specimens with post-cure (group TCPC and 50PC to 350PC) were made from samples of the group TC and the groups 50 to 350 cured as described here above and then post-cured in an oven at 160 °C under 0.1 MPa for 1 h.

### 2.2. Conversion degree

Ten specimens (19 mm × 12 mm × 1 mm) made from each PICN groups were polished with a 2400 grit silicon carbide (SiC) paper on a water-irrigated grinding wheel. After drying, they were placed in a metal holder between two glasscover slips. Samples for the determination of the DC had dimensions of 19 mm × 12 mm × 1 mm in order to be place in the sample carrier (metal holder with two glasscover slips) of the spectrometer apparatus. The measurements of DC were done using Nicolet IS10 FT-IR (Thermo Scientific, Madison, WI, USA) spectrometer

**Table 1**
Group, polymerization, post-polymerization parameters and results (Mean ± SD) of conversion degree (n = 10), storage modulus (E') (n = 8), loss modulus (E") (n = 8), tan δ (n = 8), and $T_g$ (n = 8), along with results of statistical analyses [#]. All materials were synthetized by Majeb SPRL, with polymer of urethane dimethacrylate (CAS: 72869-86-4), VITA Mark II as filler ($V_f$ =73.8%) which is feldspathic ceramic reinforced with albite nepheline and 0.5% benzoyl peroxide as initiator.

| Group | Polymerization parameters | Post-curing parameters | Conversion degree (%) | E' (GPa) | E'' (GPa) | tan δ | $T_g$ (°C) |
|---|---|---|---|---|---|---|---|
| TC | 90 °C, 0.1 MPa for 4 h | none | 81.60 ± 1.10 $^{h}$ | 17.40 ± 1.34 $^{cd}$ | 1.12 ± 0.13 $^{ab}$ | 0.064 ± 0.004 $^{ab}$ | 103.61 ± 2.83 $^{g}$ |
| TCPC | 90 °C, 0.1 MPa for 4 h | 160 °C 1 h | 95.33 ± 0.45 $^{bc}$ | 19.17 ± 1.31 $^{abcd}$ | 1.12 ± 0.07 $^{ab}$ | 0.058 ± 0.003 $^{b}$ | 138.04 ± 1.46 $^{a}$ |
| 50 | 90 °C, 50 MPa for 4 h | none | 88.47 ± 1.73 $^{g}$ | 18.62 ± 1.67 $^{abcd}$ | 1.16 ± 0.09 $^{ab}$ | 0.062 ± 0.004 $^{ab}$ | 109.56 ± 1.47 $^{f}$ |
| 50PC | 90 °C, 50 MPa for 4 h | 160 °C 1 h | 96.90 ± 0.56 $^{ab}$ | 16.85 ± 1.13 $^{d}$ | 0.97 ± 0.09 $^{b}$ | 0.058 ± 0.004 $^{b}$ | 133.19 ± 1.53 $^{bc}$ |
| 100 | 90 °C, 100 MPa for 4 h | none | 94.59 ± 0.29 $^{cd}$ | 20.04 ± 0.96 $^{abc}$ | 1.15 ± 0.14 $^{ab}$ | 0.057 ± 0.006 $^{b}$ | 134.71 ± 0.79 $^{ab}$ |
| 100PC | 90 °C, 100 MPa for 4 h | 160 °C 1 h | 96.52 ± 0.22 $^{abc}$ | 19.02 ± 1.28 $^{abcd}$ | 1.02 ± 0.10 $^{b}$ | 0.054 ± 0.003 $^{b}$ | 119.66 ± 1.51 $^{e}$ |
| 150 | 90 °C, 150 MPa for 4 h | none | 94.57 ± 0.30 $^{cd}$ | 21.24 ± 0.34 $^{a}$ | 1.12 ± 0.05 $^{ab}$ | 0.053 ± 0.003 $^{b}$ | 134.69 ± 0.36 $^{ab}$ |
| 150PC | 90 °C, 150 MPa for 4 h | 160 °C 1 h | 97.16 ± 0.11 $^{ab}$ | 20.45 ± 0.98 $^{a}$ | 1.15 ± 0.14 $^{ab}$ | 0.056 ± 0.009 $^{b}$ | 124.43 ± 0.82 $^{d}$ |
| 200 | 90 °C, 200 MPa for 4 h | none | 93.01 ± 0.59 $^{de}$ | 20.55 ± 0.75 $^{a}$ | 1.22 ± 0.18 $^{ab}$ | 0.059 ± 0.007 $^{b}$ | 131.60 ± 0.29 $^{bc}$ |
| 200PC | 90 °C, 200 MPa for 4 h | 160 °C 1 h | 97.13 ± 0.37 $^{ab}$ | 19.02 ± 0.76 $^{abcd}$ | 1.05 ± 0.08 $^{ab}$ | 0.055 ± 0.004 $^{b}$ | 133.00 ± 1.49 $^{bc}$ |
| 250 | 90 °C, 250 MPa for 4 h | none | 92.40 ± 0.39 $^{ef}$ | 20.45 ± 0.70 $^{a}$ | 1.12 ± 0.08 $^{ab}$ | 0.055 ± 0.003 $^{b}$ | 129.86 ± 0.54 $^{c}$ |
| 250PC | 90 °C, 250 MPa for 4 h | 160 °C 1 h | 97.35 ± 0.22 $^{ab}$ | 18.89 ± 1.10 $^{abcd}$ | 1.04 ± 0.09 $^{ab}$ | 0.055 ± 0.004 $^{a}$ | 122.21 ± 0.92 $^{de}$ |
| 300 | 90 °C, 300 MPa for 4 h | none | 90.43 ± 0.70 $^{fg}$ | 20.37 ± 0.85 $^{a}$ | 1.14 ± 0.11 $^{ab}$ | 0.056 ± 0.004 $^{b}$ | 123.84 ± 1.32 $^{d}$ |
| 300PC | 90 °C, 300 MPa for 4 h | 160 °C 1 h | 97.73 ± 0.38 $^{a}$ | 20.37 ± 1.40 $^{a}$ | 1.07 ± 0.05 $^{ab}$ | 0.053 ± 0.004 $^{b}$ | 123.20 ± 1.64 $^{de}$ |
| 350 | 90 °C, 350 MPa for 4 h | none | 75.37 ± 2.64 $^{i}$ | 17.60 ± 0.84 $^{bcd}$ | 1.31 ± 0.10 $^{a}$ | 0.074 ± 0.006 $^{a}$ | 94.06 ± 2.17 $^{h}$ |
| 350PC | 90 °C, 350 MPa for 4 h | 160 °C 1 h | 96.31 ± 0.47 $^{abc}$ | 20.16 ± 1.01 $^{ab}$ | 1.12 ± 0.07 $^{ab}$ | 0.056 ± 0.003 $^{b}$ | 134.81 ± 0.95 $^{ab}$ |

# The same superscript letters demonstrate no significant difference for respective property. (Scheffé test, $p > 0.05$).

Transmission NIR. NIR source 714–016300 (Thermo Scientific, Madison, WI, USA) was chosen instead of the Mid IR because of its higher sensitivity. The spectra were recorded with 384 scans at a 2 $cm^{-1}$ resolution and absorbance of the fully resolved methacrylate (=C–H) first overtone absorption centered at 6164 $cm^{-1}$. DC was calculated by using the following equation:

$$\%conversion = \left(1 - \frac{P}{M}\right) \times 100$$

where $P$ and $M$ are the area of the = C–H PICN polymer and PICN monomer peaks respectively.

Transmission near infrared spectroscopy technique was used in this study for the same reason as the previous one (Phan et al., 2015). Stansbury et al. and the Academy of Dental Material Guidance highlighted the possibility to determine the DC in the NIR bands (=CH absorption peak centered at 6164 $cm^{-1}$) (Ferracane et al., 2017; Stansbury and Dickens, 2001), in transmission with 3 mm thick samples (Stansbury and Dickens, 2001) and to have similar results as in the MID-IR IR (C=C absorption peak centered at 1637 $cm^{-1}$). Further transmission technique using a Nicolet IS-10 FTIR has been shown to be a reliable method to determine DC (Phan et al., 2015). Contrarily to the present study NIR source was used in place of IR source in order to enhance the signal. 1 mm thick sample was used instead of 3 mm as described by Stansbury et al. and applied in previous study. Thus, compared to UDMA polymer, fillers in PICN composition led to a less translucent material and interfered with the beam. That is why reducing thick sample was necessary and 1 mm thick sample permitted to obtain optimum compromise between signal and disturbance.

### 2.3. Dynamic mechanical analysis

One part of each polymerized PICN blocks obtained was cut with a low-speed Isomet saw (Buehler, Lake Bluff, Il, USA) under water irrigation into 20 rectangular specimens (4 mm × 20 mm × 1 mm) from which eight were randomly selected then polished on an 800-grit SiC paper on a water-irrigated grinding wheel and stored at room temperature under dry conditions. Their viscoelastic properties were determined using dynamic mechanical analysis (DMA) (Menard, 2008) in three-point bending mode using a Thermal Analysis Controller 7/DX instrument (PerkinElmer, Waltham, MA, USA). A static load of 2.5 ± 0.02 N was applied. The dynamic load was applied in the form of a sinusoidal strain with the corresponding static load being 10% higher than the dynamic load. The experiments were strain-controlled and maximum flexural strain was maintained at 0.05% for the entire set of experiments. Measurements were carried out using a 2 °C $min^{-1}$ heating ramp from 30 to 180 °C at a frequency of 1 Hz and a 15 mm spread of the three-point bending arrangement. Those measurements allowed the determination of storage modulus (E′ at 32 °C), loss modulus (E″ at 32 °C), and damping factor at 32 °C (tan δ) described in previous studies (Béhin et al., 2014; Phan et al., 2015). The dimensions of each sample were measured with a digital calliper (Mitutoyo Co, Kawasaki, Japan) before testing.

### 2.4. Statistical analysis

The results of DC and viscoelastic properties (E′, E″, tan δ and $T_g$) for all groups were analyzed by one-way analysis of variance (ANOVA) ($\alpha = 0.05$). The effects of pressure polymerization and post-cure on DC and viscoelastic properties (E′, E″, $T_g$ and tan δ) were analyzed by two-way analysis of variance (ANOVA) ($\alpha = 0.05$). One-way and two-way ANOVA were followed, if warranted, by Scheffé multiple-mean comparisons ($\alpha = 0.05$), using PASW Statistics 18.

Pearson's tests ($\alpha = 0.05$) were used to verify the presence of statistically significant correlations between DC and viscoelastic properties.

## 3. Results

The results of DC and DMA characterization with the statistical analyses are summarized in Table 1 and are given in Fig. 1 (a)-(e) and 2 (a)-(b).

Two-way ANOVA analysis for DC, E', E", tan δ and $T_g$ are shown in Table 2 for varying pressure polymerized (0.1 MPa–350 MPa) and with/without PC.

### 3.1. Conversion degree

PICN obtained via high pressure polymerization (groups 50 to 300) had higher DC than those of control group (TC). DC of group 350 was lower than those of control group (TC). Among the high pressure groups without PC, the increase in pressure from 0.1 MPa to 100 MPa resulted in an increase in DC and a decrease in DC above 150 MPa. PC significantly increased DC for each group except for group 100 where DC was already close to its maxima prior to post curing.

### 3.2. Dynamic mechanical characterization

The results for loss modulus (E") have shown no significant difference between the control group (TC) and experimental high pressure

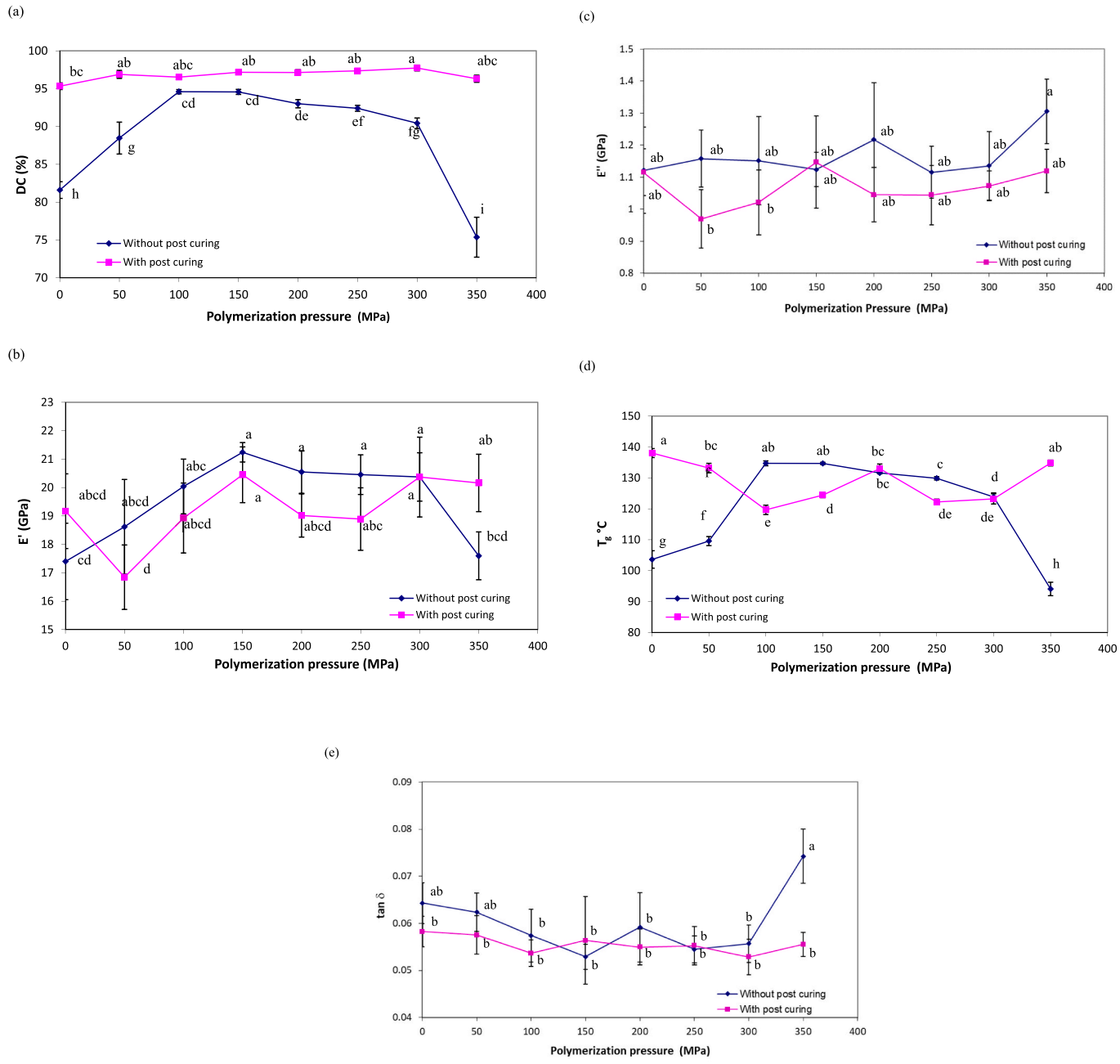


**Fig. 1.** (a) Conversion degree (n = 10); (b) Storage modulus E' (n = 8); (c) Loss modulus E'' (n = 8); (d) Glass transition temperature $T_g$ (n = 8); (e) Damping factor tan δ (n = 8). The results are expressed as the means ± SD.The same superscript letters demonstrate that there were no significant differences for each factor (1-way analysis of variance followed by Scheffé test, α = 0.05).

polymerized polymers.

E′ and $T_g$ for without PC groups presented the same trend: they increased with the increase of pressure until 150 MPa and 100 MPa respectively. Then the values reached a plateau between 150 MPa and 300 MPa for E' and between 100 MPa and 300 MPa for $T_g$. Finally, these values decreased for higher pressures in link with DC changes (see later).

The damping factor (tan δ) of 350 group was higher than for the control group (TC). Regarding $T_g$, PC promoted higher $T_g$ at 0.1 MPa, 50 MPa and 350 MPa while it decreased $T_g$ at 100 MPa, 150 MPa and 250 MPa.

Two-way ANOVA analysis (Table 2) showed that PC has not induced significant differences for E'. However, it involved a decrease of both E″ and tan δ. Significant differences ($p < 0.05$) were also noted in the effect of pressure and pressure/PC combined on DC, E′, E″, tan δ and $T_g$. Thus, significant differences ($p < 0.05$) were observed for the effect of PC on DC, E", tan δ and $T_g$. Optimum polymerization parameters seemed to be 100–150 MPa without PC. Among groups with PC, highest DC and E' were obtained with 300PC group and optimum $T_g$ with 200 PC group.

Pearson's correlation coefficient revealed a strong and significant ($p < 0.05$) correlation only between DC and E' (R = 0.90), between DC and $T_g$ (R = 0.96), and between $T_g$ and E' (R = 0.94) for PICN without PC. These positive correlations ($R^2 = 0.812$, $R^2 = 0.928$ respectively and $R^2 = 0.889$, see Fig. 2 (a)-(b)) suggested that over 81% of the variation in E′, over 92% of the variation in $T_g$ were explained by DC, and over 88% of the variation in E′ were explained by $T_g$. Contrariwise Pearson's correlation coefficient revealed no correlation for DC and their viscoelastic properties for groups with PC. Based on the results, the null hypothesis of no effect of high pressure and PC on DC and viscoelastic properties (E′,

**Table 2**
Two-way analysis of variance (ANOVA) for conversion degree and viscoelastic properties.

| Conversion Degree (%) | | | | | | | |
|---|---|---|---|---|---|---|---|
| Factor | | Mean ± SD # | df | Type III sum of squares | Mean square | F | significance |
| P: Pressure (MPa) | 0.1 (thermocured) | 88.46 ± 7.09 $^{d}$ | 7 | 1907.394 | 272.485 | 327.512 | * |
| | 50 | 92.68 ± 4.5 $^{c}$ | | | | | |
| | 100 | 95.55 ± 1.02 $^{a}$ | | | | | |
| | 150 | 95.87 ± 1.35 $^{a}$ | | | | | |
| | 200 | 95.07 ± 2.16 $^{ab}$ | | | | | |
| | 250 | 94.88 ± 2.56 $^{ab}$ | | | | | |
| | 300 | 94.08 ± 3.79 $^{b}$ | | | | | |
| | 350 | 85.84 ± 10.9 $^{e}$ | | | | | |
| PC: post-cure | Without PC | 88.8 ± 6.59 $^{b}$ | 1 | 2559.171 | 2559.171 | 3075.983 | * |
| | With PC | 96.8 ± 0.79 $^{a}$ | | | | | |
| P*PC | (Table 1 columns Group and conversion degree) | | 7 | 1456.662 | 208.095 | 250.118 | * |
| E' (GPa) | | | | | | | |
| Factor | | Mean ± SD # | df | Type III sum of squares | Mean square | F | significance |
| P: Pressure (MPa) | 0.1 (thermocured) | 18.28 ± 1.58 $^{cd}$ | 7 | 121.067 | 17.295 | 14.942 | * |
| | 50 | 17.73 ± 1.65 $^{d}$ | | | | | |
| | 100 | 19.53 ± 1.21 $^{abc}$ | | | | | |
| | 150 | 20.84 ± 0.98 $^{a}$ | | | | | |
| | 200 | 19.78 ± 1.08 $^{ab}$ | | | | | |
| | 250 | 19.67 ± 1.2 $^{abc}$ | | | | | |
| | 300 | 20.37 ± 1.12 $^{a}$ | | | | | |
| | 350 | 18.88 ± 1.6 $^{bcd}$ | | | | | |
| PC: post-cure | Without PC | 19.53 ± 1.67 $^{a}$ | 1 | 2.752 | 2.752 | 2.378 | – |
| | With PC | 19.24 ± 1.54 $^{a}$ | | | | | |
| P*PC | (Table 1 columns Group and E') | | 7 | 74.456 | 10.637 | 9.189 | * |
| E'' (GPa) | | | | | | | |
| Factor | | Mean ± SD # | df | Type III sum of squares | Mean square | F | significance |
| P:Pressure (MPa) | 0.1 (thermocured) | 1.12 ± 0.10 $^{ab}$ | 7 | 0.239 | 0.034 | 3.133 | * |
| | 50 | 1.06 ± 0.13 $^{b}$ | | | | | |
| | 100 | 1.09 ± 0.14 $^{ab}$ | | | | | |
| | 150 | 1.14 ± 0.11 $^{ab}$ | | | | | |
| | 200 | 1.13 ± 0.16 $^{ab}$ | | | | | |
| | 250 | 1.08 ± 0.09 $^{ab}$ | | | | | |
| | 300 | 1.10 ± 0.09 $^{ab}$ | | | | | |
| | 350 | 1.21 ± 0.13 $^{a}$ | | | | | |
| PC: post-cure | Without PC | 1.17 ± 0.13 $^{a}$ | 1 | 0.316 | 0.316 | 28.953 | * |
| | With PC | 1.07 ± 0.10 $^{b}$ | | | | | |
| P*PC | (Table 1 columns Group and E'') | | 7 | 0.190 | 0.27 | 2.487 | * |
| tan δ | | | | | | | |
| Factor | | Mean ± SD # | df | Type III sum of squares | Mean square | F | significance |
| P: Pressure (MPa) | 0.1 (thermocured) | 0.061 ± 0.005 $^{ab}$ | 7 | 0.002 | 0.0002 | 10.536 | * |
| | 50 | 0.060 ± 0.005 $^{abc}$ | | | | | |
| | 100 | 0.056 ± 0.005 $^{bc}$ | | | | | |
| | 150 | 0.055 ± 0.007 $^{c}$ | | | | | |
| | 200 | 0.057 ± 0.006 $^{bc}$ | | | | | |
| | 250 | 0.055 ± 0.003 $^{bc}$ | | | | | |
| | 300 | 0.054 ± 0.004 $^{c}$ | | | | | |
| | 350 | 0.065 ± 0.011 $^{a}$ | | | | | |
| PC: post-cure | Without PC | 0.060 ± 0.008 $^{a}$ | 1 | 0.001 | 0.0006 | 29.065 | * |
| | With PC | 0.056 ± 0.005 $^{b}$ | | | | | |
| P*PC | (Table 1 columns Group and tanδ) | | 7 | 0.001 | 0.0002 | 7.613 | * |
| $T_g$ (°C) | | | | | | | |
| Factor | | Mean ± SD # | Df | Type III sum of squares | Mean square | F | significance |
| P: Pressure (MPa) | 0.1 (thermocured) | 120.83 ± 17.9 $^{e}$ | 7 | 3542.390 | 506.056 | 254.470 | * |
| | 50 | 121.38 ± 12.29 $^{e}$ | | | | | |
| | 100 | 127.19 ± 7.86 $^{c}$ | | | | | |
| | 150 | 129.56 ± 5.33 $^{b}$ | | | | | |
| | 200 | 132.30 ± 1.26 $^{a}$ | | | | | |
| | 250 | 126.04 ± 4.02 $^{c}$ | | | | | |
| | 300 | 123.52 ± 1.48 $^{d}$ | | | | | |
| | 350 | 114.44 ± 21.11 $^{f}$ | | | | | |
| PC: post-cure | Without PC | 120.24 ± 14.88 $^{b}$ | 1 | 2217.447 | 2217.447 | 1115.043 | * |
| | With PC | 128.57 ± 6.64 $^{a}$ | | | | | |
| P*PC | (Table 1 columns Group and $T_g$) | | 7 | 12968.835 | 1852.691 | 931.626 | * |

*: significant difference was detected($p < 0.05$).
# The same superscript letters demonstrate no significant difference for respective property and factor. (Scheffé test, $p > 0.05$).

(a)

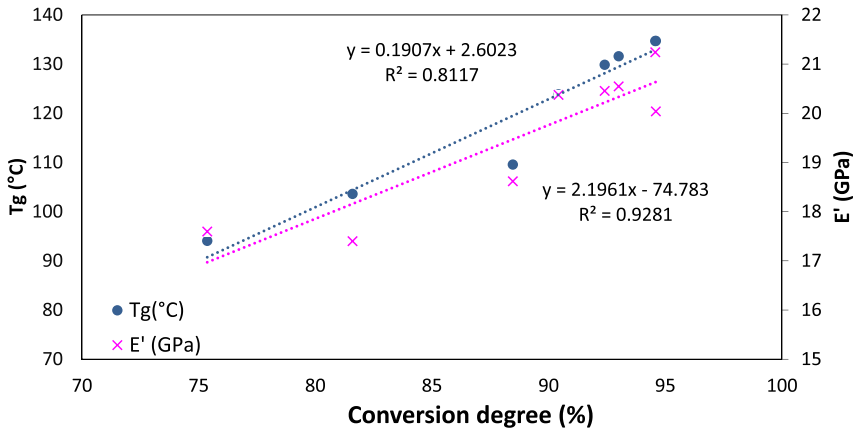


(b)

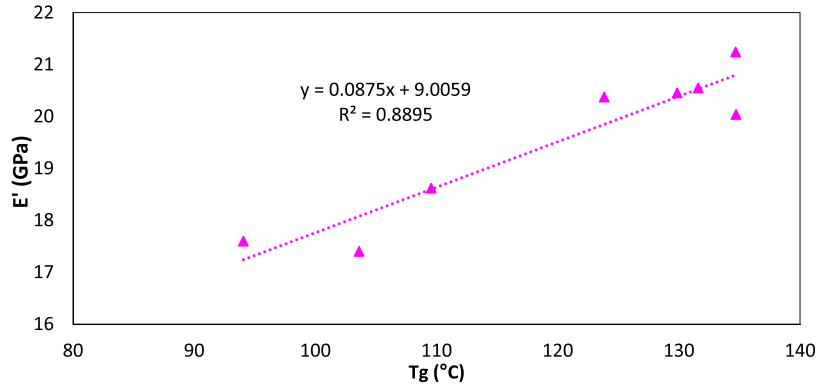


**Fig. 2.** (a) Correlations of conversion degree with E' ($R^2 = 0.812$), and conversion degree with $T_g$ ($R^2 = 0.928$) for groups without PC. (b) Correlation of $T_g$ with E' ($R^2 = 0.889$) for groups without PC.

E″, tan δ and $T_g$) is rejected.

## 4. Discussion

The purpose of this study is to characterize the influence of pressure polymerization and post-cure on DC, viscolelastic properties and to determine the optimal polymerization parameters. In view of the above findings, the null hypothesis that varying polymerization pressure and PC have no effect on DC and on the viscoelastic properties is rejected.

The significant impact of high pressure polymerization on DC and viscoelastic properties, shown in this study, corroborates earlier reports on the influence of pressure on polymerization kinetics of polymer (Arita et al., 2008; Kaminski et al., 2008; Kojima et al., 2002; Schettino et al., 2008) which also explain the trends presented in Table 1, and an optimum pressure of 100–150 MPa for DC and $T_g$ concerning groups without PC. Thus, it was observed experimentally a strong correlation between DC and $T_g$ ($R^2 = 0.928$) as depicted in Fig. 2 (a)–(b) for groups without PC. Indeed relation between the $T_g$ and DC, and using $T_g$ as an index of progress of cure (DiBenedetto, 1987; Kato et al., 2020; Lovell et al., 2001; Pascault and Williams, 1990) and between $T_g$ and E' have been reported (Sanditov et al., 2012).

Regarding the influence of pressure of polymerization on E′, the same trend could be noticed as for DC or $T_g$. High pressure polymerization did not influence E′ of pure UDMA polymer (Phan et al., 2015) because the bulk modulus in glassy state depends on cohesive energy density (Pascault et al., 2002) and is barely influenced by conversion degree in the range under investigation (Pomes et al., 2018). However, a positive influence of high pressure on E′ was noticed and a high correlation were observed between DC and E' ($R^2 = 0.812$) and between E' and $T_g$ ($R^2 = 0.889$) (Fig. 2 (a)–(b)).

A proposed explanation for the strong effect in the case of PICN composite blocks is that the observed increase is due to the specific contribution of interface, where silano-acrylate groups react to the coupling matrix and fillers and later ensures a better stiffness, meaning that compatibilizer groups has a great influence on the overall mechanical behavior. In other words, pressure variation and also DC would have concerned the reactivity of the C═C double bond of the silane and thus the bonding between the polymer matrix and fillers. That could explain correlation between DC and E'.

Optimal polymerization parameter is 100–150 MPa without PC and values of DC, $T_g$ and E' are respectively at 94%, 134 °C and 20.0–21.2 GPa. The obtained high values of DC allow positive effects increasing mechanical properties, decreasing free monomers leaching as previously reported (Asmussen and Peutzfeldt, 1998; Par et al., 2019; Soares et al., 2005). On the other hand, higher DC could result in adverse effects such as increased internal stress and volumetric shrinkage which induces interfacial gap formation at margin resulting in microleakage, in case of photopolymerized direct composites (Ferracane, 2005; Leprince et al.,

2013). Nevertheless, CAD/CAM composite blocks allow to overcome these negative effects of higher DC. Thus, CAD/CAM composite blocks are prepolymerized, their polymerization taking place during their industrial manufacturing, so that shrinkage stress is not induced at margin. HP polymerization process could also decrease volumetric shrinkage and so internal stress by reducing monomers distance (Kojima et al., 2002).

Besides, DC increases up to 97.7% with PC which has a positive impact as expected (Par et al., 2019). Indeed, as the chain propagation takes place successively in three steps leading to the formation of a network: a pre-gel or liquid step, a gel step (viscoelastic) and a glassy step (Rey et al., 2002). The transition to glassy step, or vitrification, corresponds to the transition from a viscoelastic gel to a glassy solid state. This latter is characterized by a drop of the molecular mobility so that propagation polymerization reaction is no longer possible. This explains why in the present study the DC never reaches 100% (Leprince et al., 2013; Lovell et al., 1999) despite of high pressure polymerization. That is the reason why a PC treatment is used so as to make possible the reaction of the residual C═C double bonds. Consequently, PC allows to pursue the polymerization and an increase in DC up to a max of 95–97% for all PICN regardless of their polymerization pressure. For that purpose, a PC temperature higher than the $T_g$ of PICN was needed.

It is to highlight that increasing in DC is higher with groups with lower DC after high pressure polymerization (groups TC and 350) than those with better DC (groups 100, 150, 200, 250). Thus, PC leads to a dramatic increase in $T_g$ for groups TC and 350 while $T_g$ decreases or is unchanged for 100, 150, 200, 250 groups. Besides, the increase in mechanical properties due to PC reported in previous studies were obtained with conventionally photopolymerized composites which had low DC (55–69%) (Al-Ahdal et al., 2015; Ferracane, 2011).

However, this increase in DC due to PC is followed by a decrease in $T_g$ at 150 MPa pressure polymerization. In fact, PC seems to have contradictious effects on the $T_g$, depending on the DC obtained after the first high pressure polymerization stage and the gain in DC after PC. On the one hand, PC allows the increase of the DC which results in increased crosslinking density and also higher $T_g$ (Li and Strachan, 2016; Lovell et al., 2001). On the other hand, it is possible that methacrylate nodes depolymerized after heat exposure. It is for example well established that PMMA polymer can self-degrade under inert atmosphere (Kaminsky et al., 2004), because of the steric hindrance of methacrylate groups and subsequent low C–C bond dissociation energy (Roberts, 1950). In other words, PICN under study would be in a very narrow region comprised between vitrification and degradation in the Time Temperature Transformation diagram (Vidil et al., 2016) but this remains to be formerly established in the case of PICN. As lower $T_g$ could have a negative impact on mechanical properties, studies are necessary to investigate influence of pressure polymerization and PC on mechanical properties of PICN. Thus, overall effect of PC on viscoelastic properties seems to be a balance between a gain in DC towards a loss due to polymer degradation regarding the results.

At this optimal polymerization parameter, E' (20.0–21.2 GPa) presents advantageous values. Indeed, E′ of enamel and dentin are reported to be between respectively 63 GPa and 14–31 GPa (Halvorson et al., 2003; Yi et al., 2020). Thus E′ of experimental PICN at the optimal polymerization parameters (20.0–21.1 GPa) are similar to E′ of dentin while E′ of commercial dispersed fillers composite blocks such as Cerasmart (8.8 GPa) or Lava Ultimate (14.9 GPa) (Al-shatti et al., 2019) and E′ of commercial conventional photopolymerized composite (4.0–7.0 GPa) (Vouvoudi and Sideridou, 2012; Yap et al., 2020) are lower. E' of commercial PICN (Enamic) was measured at 36.1 GPa. Moreover, PICN microstructure with its interpenetrating network allows to produce functionally graded blocks with elastic modulus (27.2–41.9 GPa) close to both those of enamel and dentin tissues (M. Eldafrawy et al., 2018). Elastic modulus has a key importance for materials aimed at dental restorations purposes. Indeed differences in E between tooth and restoration materials influenced the stress concentration at the bonding interface leading to interface debonding, microleakage, secondary caries and so failure (Al-shatti et al., 2019; Trindade et al., 2018). Dental restorations milled from PICN blocks could also allow better longevity of dental restorations than dispersed fillers resin composite restorations. Thus, damping factor (tan δ) expressing the capacity to dissipate energy from occlusal and masticatory loads of experimental PICN are similar to those of commercial composite blocks (Cerasmart, Lava Ultimate).

Besides, impact of the microstructure of PICN with glass ceramic network on kinetic polymerization, and so DC and $T_g$ can be highlighted. In this study, experimental PICN were cured at a 90 °C temperature which allows to compare the results of the present study to those of Phan and al's one where DC and viscoelastic properties of pure UDMA polymerized at same conditions (90 °C and various pressure from 0.1 MPa to 350 MPa) were determined. Consequently, the influence of the glass ceramic network of PICN on DC and viscoelastic properties could be discussed compared to polymer of pure UDMA. In a previous study (Phan et al., 2015), DC and $T_g$ of UDMA polymers reached a plateau from 200 MPa to 350 MPa contrarily to results of the present study in which $T_g$ and DC of PICN (without PC) decreased beyond 250 MPa. This suggests a possible impact of fillers (glass ceramic network) on polymerization rate. First, fillers possibly inhibited the mobility of reactive mixture and subsequent DC and $T_g$ (Halvorson et al., 2003; Leprince et al., 2013; Tanimoto et al., 2005). Moreover, exothermal reaction of PICN was lower than for UDMA polymer as the presence of glass ceramic network (Vf = 73.8%) induced a volume fraction of UDMA resin 4 times lower in a PICN than in a pure UDMA polymer. Thus, the ceramic network could have absorbed, to a lesser extent, a part of the heat released by the exothermal polymerization (Karatas et al., 2015). That could explain decrease in polymerization rate and subsequent DC and $T_g$ of PICN beyond 250 MPa.

## 5. Conclusions

The results of the current study, based on both DC results and the DMA characterization, show that high pressure polymerization improves significantly DC, E' and $T_g$ of PICN with an optimum at 100–150 MPa, 90 °C, without PC. DC and viscoelastic properties of PICN suggest that this material is well suited for dental restoration applications.

## CRediT authorship contribution statement

**Benjamin Pomès:** Writing - original draft, Investigation. **Pascal Behin:** Writing - review & editing, Investigation. **Laurence Jordan:** Writing - review & editing. **Stéphane Legoff:** Resources. **Gregory Stoclet:** Writing - review & editing. **Emmanuel Richaud:** Conceptualization, Writing - original draft. **Jean-François Nguyen:** Conceptualization, Investigation, Formal analysis, Writing - original draft.

## Declaration of competing interest

The authors declare that they have no known competing financial interests or personal relationships that could have appeared to influence the work reported in this paper.


## Acknowledgment

Dr Michael Sadoun (Majeb, Liege) is gratefully acknowledged for his help in PICN synthesis.


## References


Al-Ahdal, K., Ilie, N., Silikas, N., Watts, D.C., 2015. Polymerization kinetics and impact of post polymerization on the Degree of Conversion of bulk-fill resin-composite at clinically relevant depth. Dent. Mater. 31, 1207–1213. https://doi.org/10.1016/j.dental.2015.07.004.

Al-shatti, R.A., Dashti, G.H., Philip, S., Michael, S., Swain, M.V., Cam, C.A.D., 2019. Size or hierarchical dependence of the elastic modulus of three ceramic-composite CAD/CAM materials. Dent. Mater. 35, 953–962. https://doi.org/10.1016/j.dental.2019.03.012.

Almeida-chetti, V.A., Macchi, R.L., Iglesias, M.E., 2014. Effect of post-curing treatment on mechanical properties of composite. Resins 27, 72–76. https://doi.org/10.1590/S1852-48342014000200005.

Arita, T., Kayama, Y., Ohno, K., Tsujii, Y., Fukuda, T., 2008. High-pressure atom transfer radical polymerization of methyl methacrylate for well-defined ultrahigh molecular-weight polymers. Polymer 49, 2426–2429. https://doi.org/10.1016/j.polymer.2008.03.026.

Asmussen, E., Peutzfeldt, A., 1998. Influence of UEDMA, BisGMA and TEGDMA on selected mechanical properties of experimental resin composites. Dent. Mater. 14, 51–56. https://doi.org/10.1016/S0109-5641(98)00009-8.

Asmussen, E., Peutzfeldt, A., 1990. Mechanical properties of heat treated restorative resins for use in the inlay/onlay technique. Eur. J. Oral Sci. 98, 564–567. https://doi.org/10.1111/j.1600-0722.1990.tb01013.x.

Bandarra, S., Mascarenhas, P., Luís, A.R., Catrau, M., Bekman, E., Ribeiro, A.C., Félix, S., Caldeira, J., Barahona, I., 2020. In vitro and in silico evaluations of resin-based dental restorative material toxicity. Clin. Oral Invest. 24, 2691–2700. https://doi.org/10.1007/s00784-019-03131-4.

Barutcigil, K., Dündar, A., Batmaz, S.G., Yıldırım, K., Barutçugil, Ç., 2020. Do resin-based composite CAD/CAM blocks release monomers? Clin. Oral Invest. https://doi.org/10.1007/s00784-020-03377-3.

Béhin, P., Stoclet, G., Ruse, N.D., Sadoun, M., 2014. Dynamic mechanical analysis of high pressure polymerized urethane dimethacrylate. Dent. Mater. 30, 728–734. https://doi.org/10.1016/j.dental.2014.04.002.

Bouillaguet, S., 2004. Biological risks of resin-based materials to the dentin-pulp complex. Crit. Rev. Oral Biol. Med. 15, 47–60. https://doi.org/10.1177/154411304015001050.

Cândea Ciurea, A., Şurlin, P., Stratul, Ş.I., Soancă, A., Roman, A., Moldovan, M., Tudoran, B.L., Pall, E., 2019. Evaluation of the biocompatibility of resin composite-based dental materials with gingival mesenchymal stromal cells. Microsc. Res. Tech. 82, 1768–1778. https://doi.org/10.1002/jemt.23343.

Coldea, A., Swain, M.V., Thiel, N., 2013. Mechanical properties of polymer-infiltrated-ceramic-network materials. Dent. Mater. 29, 419–426. https://doi.org/10.1016/j.dental.2013.01.002.

de Paula Silveira, A.C., Chaves, S.B., Hilgert, L.A., Ribeiro, A.P.D., 2017. Marginal and internal fit of CAD-CAM-fabricated composite resin and ceramic crowns scanned by 2 intraoral cameras. J. Prosthet. Dent 117, 386–392. https://doi.org/10.1016/j.prosdent.2016.07.017.

DiBenedetto, A.T., 1987. Prediction of the glass transition temperature of polymers: a model based on the principle of corresponding states. J. Polym. Sci., Part B: Polym. Phys. 25, 1949–1969. https://doi.org/10.1002/polb.1987.090250914.

Eldafrawy, M., Ebroin, M., Gailly, P., Nguyen, J., Sadoun, M., Mainjot, A., 2018a. Bonding to CAD-CAM composites: an interfacial fracture toughness approach. J. Dent. Res. 97, 60–67. https://doi.org/10.1177/0022034517728714.

Eldafrawy, M., Greimers, L., Bekaert, S., Gailly, P., Lenaerts, C., Nguyen, J.F., Sadoun, M., Mainjot, A., 2019. Silane influence on bonding to CAD-CAM composites: an interfacial fracture toughness study. Dent. Mater. 35, 1279–1290. https://doi.org/10.1016/j.dental.2019.05.019.

Eldafrawy, M., Nguyen, J.F., Mainjot, A.K., Sadoun, M.J., 2018b. A functionally graded PICN material for biomimetic CAD-CAM blocks. J. Dent. Res. 97, 1324–1330. https://doi.org/10.1177/0022034518785364.

Ferracane, J.L., 2013. Resin-based composite performance: are there some things we can't predict? Dent. Mater. 29, 51–58. https://doi.org/10.1016/j.dental.2012.06.013.

Ferracane, J.L., 2011. Resin composite - state of the art. Dent. Mater. 27, 29–38. https://doi.org/10.1016/j.dental.2010.10.020.

Ferracane, J.L., 2005. Developing a more complete understanding of stresses produced in dental composites during polymerization. Dent. Mater. 21, 36–42. https://doi.org/10.1016/j.dental.2004.10.004.

Ferracane, J.L., Hilton, T.J., Stansbury, J.W., Watts, D.C., Silikas, N., Ilie, N., Heintze, S., Cadenaro, M., Hickel, R., 2017. Academy of Dental Materials guidance—resin composites: Part II—technique sensitivity (handling, polymerization, dimensional changes). Dent. Mater. 33, 1171–1191. https://doi.org/10.1016/j.dental.2017.08.188.

Finer, Y., Santerre, J., 2007. Influence of silanated filler content on the biodegradation of bisGMA/TEGDMA dental composite resins. J. Biomed. Mater. Res. 81, 75–84. https://doi.org/10.1002/jbm.a.31004.

Germscheid, W., de Gorre, L.G., Sullivan, B., O'Neill, C., Price, R.B., Labrie, D., 2018. Post-curing in dental resin-based composites. Dent. Mater. 34, 1367–1377. https://doi.org/10.1016/j.dental.2018.06.021.

Giordano, R., 2006. Materials for chairside cad/cam-produced restorationso Title. J. Am. Dent. Assoc. 137, 14–21. https://doi.org/10.14219/jada.archive.2006.0397.

Grenade, C., De Pauw-Gillet, M.C., Pirard, C., Bertrand, V., Charlier, C., Vanheusden, A., Mainjot, A., 2017. Biocompatibility of polymer-infiltrated-ceramic-network (PICN) materials with human gingival keratinocytes (HGKs). Dent. Mater. 33, 333–343. https://doi.org/10.1016/j.dental.2017.01.001.

Halvorson, R.H., Erickson, R.L., Davidson, C.L., 2003. The effect of filler and silane content on conversion of resin-based composite. Dent. Mater. 19, 327–333. https://doi.org/10.1016/S0109-5641(02)00062-3.

He, L.H., Purton, D., Swain, M., 2011. A novel polymer infiltrated ceramic for dental simulation. J. Mater. Sci. Mater. Med. 22, 1639–1643. https://doi.org/10.1007/s10856-011-4350-3.

Kaminski, K., Paluch, M., Ziolo, J., Bogoslovov, R., Roland, C.M., 2008. Crosslinking polymerization of tetraethylene glycol dimethacrylate under high pressure. J. Phys. Conf. Ser. 121, 092002 https://doi.org/10.1088/1742-6596/121/9/092002.

Kaminsky, W., Predel, M., Sadiki, A., 2004. The 42nd IUPAC microsymposium on degradation, stabilisation and recycling of polymers, and the 2nd feedstock recycling of polymers by pyrolysis in a fluidised bed. Polym. Degrad. Stabil. 85, 1045–1050. https://doi.org/10.1016/j.polymdegradstab.2003.05.002.

Karatas, O., Turel, V., Bayindir, Y., 2015. Temperature rise during polymerization of different cavity liners and composite resins. J. Conserv. Dent. 18, 431–435. https://doi.org/10.4103/0972-0707.168795.

Kato, N., Ikeda, S., Hirakawa, M., Ito, H., 2020. Correlation of the abbe number, the refractive index, and glass transition temperature to the degree of polymerization of norbornane in polycarbonate polymers. Polymers 12, 1–15. https://doi.org/10.3390/polym12112484.

Khan, A.M., Satou, N., Shintani, H., Taira, M., Wakasa, K., Yamaki, M., 1993. Effects of post-curing by heat on the mechanical properties of visible-light cured inlay composites. J. Oral Rehabil. 20, 605–614. https://doi.org/10.1111/j.1365-2842.1993.tb01647.x.

Kojima, Y., Matsuoka, T., Takahashi, H., 2002. Structure of Poly (Methyl Methacrylate) Synthesized under High Pressure, pp. 473–475. https://doi.org/10.1023/A:1015382506716.

Leprince, J.G., Palin, W.M., Hadis, M.A., Devaux, J., Leloup, G., 2013. Progress in dimethacrylate-based dental composite technology and curing efficiency. Dent. Mater. 29, 139–156. https://doi.org/10.1016/j.dental.2012.11.005.

Li, C., Strachan, A., 2016. Free volume evolution in the process of epoxy curing and its effect on mechanical properties. Polymer 97, 456–464. https://doi.org/10.1016/j.polymer.2016.05.059.

Lovell, L.G., Berchtold, K.A., Elliott, J.E., Lu, H., Bowman, C.N., 2001. Understanding the kinetics and network formation of dimethacrylate dental resins. Polym. Adv. Technol. 12, 335–345. https://doi.org/10.1002/pat.115.

Lovell, L.G., Stansbury, J.W., Syrpes, D.C., Bowman, C.N., 1999. Effects of composition and reactivity on the reaction kinetics of dimethacrylate dimethacrylate copolymerizations. Macromolecules 32, 3913–3921. https://doi.org/10.1021/ma990258d.

Mainjot, A.K., Dupont, N.M., Oudkerk, J.C., Dewael, T.Y., Sadoun, M.J., 2016. From artisanal to CAD-CAM blocks. J. Dent. Res. 95, 487–495. https://doi.org/10.1177/0022034516634286.

Menard, K.P., 2008. Dynamic Mechanical Analysis – a Practical Introduction. FL: CRC Press, Boca Raton.

Miyazaki, T., Hotta, Y., Kunii, J., Kuriyama, S., Tamaki, Y., 2009. A review of dental CAD/CAM: current status and future perspectives from 20 years of experience. Dent. Mater. J. 28, 44–56. https://doi.org/10.4012/dmj.28.44.

Nguyen, J.F., Ruse, D., Phan, A.C., Sadoun, M.J., 2014. High-temperature-pressure polymerized resin-infiltrated ceramic networks. J. Dent. Res. 93, 62–67. https://doi.org/10.1177/0022034513511972.

Ong, J.E.X., Yap, A.U., Hong, J.Y., Eweis, A.H., Yahya, N.A., 2018. Viscoelastic properties of contemporary bulk-fill Restoratives : a dynamic- mechanical analysis. Operat. Dent. 43, 307–314. https://doi.org/10.2341/16-365-L.

Par, M., Marovic, D., Attin, T., Tarle, Z., Tauböck, T.T., 2020. Effect of rapid high-intensity light-curing on polymerization shrinkage properties of conventional and bulk-fill composites. J. Dent. 101 https://doi.org/10.1016/j.jdent.2020.103448.

Par, M., Spanovic, N., Tauböck, T.T., Attin, T., Tarle, Z., 2019. Degree of conversion of experimental resin composites containing bioactive glass 45S5: the effect of post-cure heating. Sci. Rep. 9 https://doi.org/10.1038/s41598-019-54035-y.

Pascault, J.P., Sautereau, H., Verdu, J., Williams, R.J.J., 2002. Thermosetting Polymers. CRC Press, New York.

Pascault, J.P., Williams, R.J.J., 1990. Glass transition temperature versus conversion relationships for thermosetting polymers. J. Polym. Sci., Part B: Polym. Phys. 28, 85–95. https://doi.org/10.1002/polb.1990.090280107.

Phan, A.C., Béhin, P., Stoclet, G., Dorin Ruse, N., Nguyen, J.F., Sadoun, M., 2015. Optimum pressure for the high-pressure polymerization of urethane dimethacrylate. Dent. Mater. 31, 406–412. https://doi.org/10.1016/j.dental.2015.01.010.

Phan, A.C., Tang, M.L., Nguyen, J.F., Ruse, N.D., Sadoun, M., 2014. High-temperature high-pressure polymerized urethane dimethacrylate - mechanical properties and monomer release. Dent. Mater. 30, 350–356. https://doi.org/10.1016/j.dental.2013.12.009.

Pomes, B., Derue, I., Lucas, A., Nguyen, J., Richaud, E., 2018. Water ageing of urethane dimethacrylate networks. Polym. Degrad. Stabil. 154, 195–202. https://doi.org/10.1016/j.polymdegradstab.2018.06.003.

Putzeys, E., Vercruyssen, C., Duca, R.C., Saha, P.S., Godderis, L., Vanoirbeek, J., Peumans, M., Van Meerbeek, B., Van Landuyt, K.L., 2020. Monomer release from direct and indirect adhesive restorations: a comparative in vitro study. Dent. Mater. 36, 1275–1281. https://doi.org/10.1016/j.dental.2020.06.001.

Rey, L., Duchet, J., Galy, J., Sautereau, H., Vouagner, D., Carrion, L., 2002. Structural heterogeneities and mechanical properties of vinyl/dimethacrylate networks synthesized by thermal free radical polymerisation. Polymer 43, 4375–4384. https://doi.org/10.1016/S0032-3861(02)00266-5.

Roberts, D., 1950. Heat of polymerization. A summary of published values and their relation to structure. J. Res. Natl. Bur. Stand. 44, 221–232.

Ruse, N.D., Sadoun, M.J., 2014. Resin-composite blocks for dental CAD/CAM applications. J. Dent. Res. 93, 1232–1234. https://doi.org/10.1177/0022034514553976.

Sadoun, M., 2011. Composite ceramic block. US patent 8 (507), 578.

Sanditov, B.D., Sangadiev, S.S., Sanditov, D.S., 2012. Relation between elastic modulus and glass softening temperature in the delocalized atom model. J. Exp. Theor. Phys. 445, 445–454. https://doi.org/10.1134/S106377611207014X.

Schettino, V., Bini, R., Ceppatelli, M., Citroni, M., 2008. Activation and control of chemical reactions at very high pressure. Phys. Scripta 78, 058104. https://doi.org/10.1088/0031-8949/78/05/058104.

Soares, C., Pizi, E., Fonseca, R., Martins, L., 2005. Mechanical properties of light-cured composites polymerized with several additional post-curing methods. Operat. Dent. 30, 389–394.

Stansbury, J.W., Dickens, S.H., 2001. Determination of double bond conversion in dental resins by near infrared spectroscopy. Dent. Mater. 17, 71–79. https://doi.org/10.1016/S0109-5641(00)00062-2.

Swain, M.V., Coldea, A., Bilkhair, A., Guess, P.C., 2016. Interpenetrating network ceramic-resin composite dental restorative materials. Dent. Mater. 32, 34–42. https://doi.org/10.1016/j.dental.2015.09.009.

Tallarico, M., 2020. Computerization and digital workflow in medicine: focus on digital dentistry. Materials 13. https://doi.org/10.3390/ma13092172.

Tanimoto, Y., Hayakawa, T., Nemoto, K., 2005. Analysis of photopolymerization behavior of UDMA/TEGDMA resin mixture and its composite by differential scanning calorimetry. J. Biomed. Mater. Res. B Appl. Biomater. 72, 310–315. https://doi.org/10.1002/jbm.b.30151.

Tassin, M., Bonte, E., Loison-Robert, L.S., Nassif, A., Berbar, T., Le Goff, S., Berdal, A., Sadoun, M., Fournier, B.P.J., 2016. Effects of high-temperature-pressure polymerized resin-infiltrated ceramic networks on oral stem cells. PloS One 11, 1–16. https://doi.org/10.1371/journal.pone.0155450.

Trindade, F.Z., Valandro, L.F., de Jage, N., Bottino, Marco Antonio Kleverlaan, C.J., 2018. Elastic properties of lithium disilicate versus feldspathic inlays: effect on the bonding by 3D finite element analysis. J. Prosthodont. 27, 741–747. https://doi.org/10.1111/jopr.12550.

Van Noort, R., 2012. The future of dental devices is digital. Dent. Mater. 28, 3–12. https://doi.org/10.1016/j.dental.2011.10.014.

Vidil, T., Tournilhac, F., Musso, S., Robisson, A., Leibler, L., 2016. Control of reactions and network structures of epoxy thermosets. Prog. Polym. Sci. 62, 126–179. https://doi.org/10.1016/j.progpolymsci.2016.06.003.

Vouvoudi, E.C., Sideridou, I.D., 2013. Effect of food/oral-simulating liquids on dynamic mechanical thermal properties of dental nanohybrid light-cured resin composites. Dent. Mater. 29, 842–850. https://doi.org/10.1016/j.dental.2013.04.013.

Vouvoudi, E.C., Sideridou, I.D., 2012. Dynamic mechanical properties of dental nanofilled light-cured resin composites : effect of food-simulating liquids. J. Mech. Behav. Biomed. Mater. 10, 87–96. https://doi.org/10.1016/j.jmbbm.2012.02.007.

Yap, A.U., Eweis, A.H., Yahya, N.A., 2020. Dynamic viscoelastic characterization of bulk-fill resin-based composites and their conventional counterparts. Operat. Dent. 45, 173–182. https://doi.org/10.2341/19-005-L.

Yi, Q., Feng, X., Zhang, C., Wang, X., Wu, X., Wang, J., Cui, F., Wang, S., 2020. Comparison of dynamic mechanical properties of dentin between deciduous and permanent teeth. Connect. Tissue Res. https://doi.org/10.1080/03008207.2020.1758684.